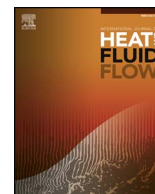




Contents lists available at ScienceDirect

## International Journal of Heat and Fluid Flow

journal homepage: [www.elsevier.com/locate/ijhff](http://www.elsevier.com/locate/ijhff)

## Reprint of: Influence of corner geometry on the secondary flow in turbulent square ducts<sup>☆, ☆ ☆</sup>

A. Vidal<sup>\*,a</sup>, R. Vinuesa<sup>b,c</sup>, P. Schlatter<sup>b,c</sup>, H.M. Nagib<sup>a</sup>

<sup>a</sup> Department of MMAE, Illinois Institute of Technology, Chicago, IL 60616, United States

<sup>b</sup> Linné FLOW Centre, KTH Mechanics SE-100 44, Stockholm, Sweden

<sup>c</sup> Swedish e-Science Research Centre (SeRC), Stockholm, Sweden

## ARTICLE INFO

## Keywords:

Wall-bounded turbulence  
Turbulent duct flow  
Corner geometry  
Secondary motions  
Direct numerical simulation

## ABSTRACT

Direct numerical simulations of fully-developed turbulent flow through a straight square duct with increasing corner rounding radius  $r$  were performed to study the influence of corner geometry on the secondary flow. Unexpectedly, the increased rounding of the corners from  $r = 0$  to 0.75 does not lead to a monotonic trend towards the pipe case of  $r = 1$ . Instead, the secondary vortices relocate close to the region of wall-curvature change. This behavior is connected to the inhomogeneous interaction between near-wall bursting events, which are further characterized in this work with the definition of their local preferential direction. We compare our results with those obtained for the flow through a square duct (which corresponds to  $r = 0$ ) and through a round pipe ( $r = 1$ ), focusing on the influence of  $r$  on the wall-shear stress distribution and the turbulence statistics along the centerplane and the corner bisector. The former shows that high-speed streaks are preferentially located near the transition between straight and curved surfaces. The Reynolds numbers based on the centerplane friction velocity and duct half-height are  $Re_{\tau_c} \approx 180$  and 350 for the cases under study.

## 1. Introduction

Streamwise corners are frequently encountered in a wide variety of engineering applications with different geometric complexities such as heat exchangers, turbo-machinery, buildings or wing roots. Turbulent flow along streamwise corners is characterized by the appearance of secondary motions of Prandtl's second kind. The secondary flow refers to the in-plane ( $y - z$ ) mean cross-flow perpendicular to the streamwise direction  $x$ . Although these motions are relatively weak compared to the streamwise velocity, they have a significant and far-reaching influence on the turbulence statistics (Bradshaw, 1987). The spanwise extension of the cross-flow was studied by Vinuesa et al. (2014, 2015b) in turbulent ducts with increasing aspect ratio  $AR$  (defined as the duct total width divided by its total height). The authors performed direct numerical simulations (DNS) at  $Re_{\tau_c} \approx 180$ , which is the friction Reynolds number based on the centerplane friction velocity and the half-height of the duct, for  $AR$  between 1 and 18, and at  $Re_{\tau_c} \approx 360$  for  $AR = 1$  and 3, using a similar numerical approach to the one presented in this study, which will be described in Section 2. Their results showed that aspect ratios larger than 10 are required for the turbulence

statistics in the duct centerplane to coincide with those present in the spanwise-periodic channel (Jiménez et al., 2004; Vinuesa et al., 2015a). Therefore, the presence of the corner affects the turbulent flow statistics throughout a large portion of the cross-sectional area around it. Although the effect of the corner geometry on the characteristics of turbulent ducts has been investigated in few studies, such as the numerical work on elliptical ducts by Nikitin and Yakhot (2005) or the simulations of hexagonal ducts by Marin et al. (2016), a systematic evaluation of such effects is not available in the literature. Thus, the goal of the present study is to perform a systematic characterization of the effects of corner geometry on the secondary flow and turbulence statistics in turbulent square duct flows, which will be discussed in detail in Sections 3 and 4 respectively. Note that an additional area where an accurate characterization of such secondary flows is critical is in turbulence modeling, since simple eddy-viscosity models, such as the  $k - \epsilon$  model, fail to properly predict the cross-flow. Therefore, the use of DNS, where all the spatial and temporal scales of turbulence are resolved, allows one to accurately capture the behavior of secondary flows, and to gain insight in order to further improve currently available RANS models.

DOI of original article: <http://dx.doi.org/10.1016/j.ijheatfluidflow.2017.07.009>

<sup>\*</sup> This article is a reprint of a previously published article. For citation purposes, please use the original publication details; Int J Heat and Fluid Flow 67A (2017), pp.69–78.

<sup>\*\*</sup> DOI of original item: [10.1016/j.ijheatfluidflow.2017.07.009](http://dx.doi.org/10.1016/j.ijheatfluidflow.2017.07.009)

<sup>\*</sup> Corresponding author.

E-mail address: [avidalto@hawk.iit.edu](mailto:avidalto@hawk.iit.edu) (A. Vidal).

<http://dx.doi.org/10.1016/j.ijheatfluidflow.2017.09.011>

Received 17 December 2016; Received in revised form 24 July 2017; Accepted 24 July 2017

0142-727X/© 2017 Elsevier Inc. All rights reserved.

In the present study, the  $90^\circ$  corner of the regular square duct is substituted by several increasing rounding radii (defined as the ratio of the radius of the corner and the half-height of the duct). The rounding radius  $r$  is a common and flexible design feature used to avoid sharp corners in the transition between two adjacent walls with different wall-tangent directions. The transition region leads to the co-existence of two surfaces with different wall curvature. In Section 3, the behavior of the turbulent flow in this transition region will be analyzed and compared with flow cases with constant wall curvature, i.e., flow through square ducts with  $90^\circ$  corners through round pipes. Note that the  $r = 0$  case corresponds to the square duct with straight corners, where the dynamics and kinematics of the secondary flow have been well documented in a number of studies, such as the ones in Refs. (Huser and Biringen, 1993; Vinuesa et al., 2015a; Uhlmann et al., 2007; Gessner, 1973; Pinelli et al., 2010; Gavrilakis, 1992) among others. Secondary motions of Prandtl's second kind consist of eight streamwise counter-rotating vortices located in pairs close to each of the corner bisectors. The cross-flow enters the corner through the bisector and leaves it through the buffer-layer region in the wall-tangent direction. Similarly, the  $r = 1$  case corresponds to the round pipe where there are no corner effects and the flow statistics are two-dimensional due to azimuthal symmetry. DNSs of turbulent pipe flow at friction Reynolds numbers (based on the pipe radius  $R$  and friction velocity  $u_\tau$ )  $Re_\tau \simeq 180, 360, 550$  and  $1000$  were performed by El Khoury et al. (2013). Therefore, the convergence from duct to pipe flow is evaluated by increasing the rounding radius of the duct.

The underlying physical mechanisms that generate the Prandtl's secondary flow of the second kind in  $r = 0$  ducts have been addressed by many authors. The secondary flow is associated with the secondary Reynolds shear-stress  $\overline{vw}$  and the anisotropy of the cross-stream deviatoric Reynolds-stress  $\overline{v^2 - w^2}$ ; e.g., see Moinuddin et al. (2004). Therefore, secondary motions of the second kind are absent in the laminar regime and flows with a wall-tangent homogeneous direction. According to Huser and Biringen (1993), secondary motions of Prandtl's second kind are generated in the near-corner region by the interaction between bursting events arising from the adjacent horizontal and vertical walls. In wall-bounded turbulent flows, these events occur periodically in the buffer-layer region exchanging momentum between the streamwise and the in-plane instantaneous velocity components. Hamilton et al. (1995) analyzed in detail the time evolution of a near-wall cycle and the relationship between the instantaneous streamwise vortices and the velocity streaks. The cycle starts with two counter-rotating streamwise vortices with rotational directions pointing in the wall-normal direction. The vortices create a mushroom-like ejection of the near-wall low-momentum fluid into the high-momentum region in the core of the flow. Then, the pair of vortices drifts apart in the spanwise direction sweeping high momentum fluid from the core of flow into the near-wall region. Therefore, ejections and sweeps are connected to low-speed and high-speed velocity streaks, respectively. Finally, the cycle repeats again with the start of two new ejections, on each side of the old ones, while shifted 100 wall units in the spanwise direction (Kline et al., 1967). Pinelli et al. (2010) showed that high-speed streaks are preferentially located in the near-corner region flanked by two low-velocity streaks on each of the perpendicular walls. These two effects prevent the instantaneous streamwise vortices near the corner from cancelling in the mean and, thus, generate the mean cross-flow. On the other hand, in pipe and channel flows the interaction and spanwise distribution of instantaneous vortices are homogeneous in the spanwise/azimuthal direction. Consequently, the instantaneous vortices cancel in the mean and no secondary motions arise. In Section 3.1, we will discuss the interaction between bursting events from walls with different curvature to shed more light into the mechanisms that produce these motions.

At low Reynolds numbers the length of the velocity streaks is of the same order of magnitude as the half-height of the duct or, in the present cases, the straight and curved surfaces of the duct, leading to

marginally-turbulent flow effects. These effects have been documented in  $r = 0$  square ducts by Uhlmann et al. (2007) and were reported Marin et al. (2016) in hexagonal ducts. They appear when the straight part of the duct is shorter than what would be needed to accommodate a complete minimal turbulent cycle (Jiménez and Moin, 1991), i.e., when less than four velocity streaks can fit simultaneously. In these cases, the short-average cross-flow consists of four streamwise vortices located in pairs at opposite walls close to the common centerplane of the walls. These vortices switch location between horizontal and vertical walls. Therefore, eight vortices appear only when statistics are obtained over long averaging intervals. Interestingly, some of the cases considered in the present study show signs of marginally-turbulent flow effects, as will be explained in subsection 3.1, due to the reduced length of the straight wall even though these are not present in the  $r = 0$  case at similar Reynolds numbers.

## 2. Numerical method

### 2.1. Description of the numerical code: Nek5000

All the rounded-corner simulations considered in the present work, including the  $r = 0$  case by Vinuesa et al. (2014) and the  $r = 1$  case by El Khoury et al. (2013), have been carried out by using the numerical code Nek5000. This code was developed by Fischer et al. (2008) at Argonne National Laboratory and is based on the spectral-element method (SEM), originally proposed by Patera (1984). The code solves the incompressible Navier–Stokes equations subject to the boundary conditions corresponding to the problem under consideration. The governing equations are cast in weak form and the spatial discretization is done by means of the Galerkin approximation, which uses the basis functions themselves as test functions. The SEM allows us to discretize the round corners using finite elements while preserving the high-order accuracy of spectral methods, which is required to properly resolve the scale disparity of turbulent flows. Within each element, the basis functions correspond to Lagrange interpolants of order  $N$  for velocity and  $N - 2$  for pressure. Thus, we will use the  $P_N - P_{N-2}$  formulation proposed by Manday and Patera (1989), where the polynomial order of the pressure is two degrees lower than the order of the velocity. Note that the velocity grid points follow the Gauss–Lobatto–Legendre (GLL) distribution. Regarding the temporal discretization, the nonlinear terms are treated explicitly by third-order extrapolation (EXT3) and the viscous terms are treated implicitly by a third-order backward differentiation scheme (BDF3). High-order splitting is used to decouple pressure and velocity. The former is obtained by solving a Poisson problem through generalized minimum residuals (GMRES), after that, one Helmholtz problem is solved for each velocity component using conjugate gradients. Nek5000 is written in Fortran77/C and employs the message-passing interface (MPI) for parallelism. The code is highly parallelizable allowing distributing the problem to thousands of processors in order to face the high computational cost associated with large-scale direct numerical simulations.

### 2.2. Description of the simulations

We performed simulations of fully-developed turbulent flow through ducts with rounding radii  $r = 0.25, 0.5$  and  $0.75$  at  $Re_\tau, c \simeq 180$  and  $r = 0.5$  at  $Re_\tau, c \simeq 350$  (where  $Re_\tau, c$  is expressed in terms of the centerplane friction velocity  $u_\tau, c$  and the duct half-height  $h$ ). The flow setup and an instantaneous visualization are shown in Fig. 1. The streamwise, vertical and spanwise directions are aligned with the  $x, y$  and  $z$  axes, respectively. The streamwise length is  $L_x = 50h$  and  $L_x = 25h$  in the  $Re_\tau, c \simeq 180$  and  $Re_\tau, c \simeq 350$  cases, respectively. The Reynolds number  $Re_b$  based on the bulk velocity  $U_b$  and  $h$  is adjusted to provide the same  $Re_\tau, c$  in the various cases. The domain has periodic boundary conditions in the homogeneous streamwise direction and no-slip boundary conditions at the walls. The pressure gradient in the

Download English Version:

<https://daneshyari.com/en/article/7053577>

Download Persian Version:

<https://daneshyari.com/article/7053577>

[Daneshyari.com](https://daneshyari.com)